Magazine of Civil Engineering

ISSN 2712-8172

journal homepage: http://engstroy.spbstu.ru/

DOI: 10.34910/MCE.107.10

Performance of structurally viable green concrete derived from natural Pozzolan and Nanosilica

***M. Ibrahim*[a] *, M. Nasir*[b], *S.R. Hussaini*[a], *S.K. Najamuddin*[a], *A.O. Ewebajo**[a]**

[a] *King Fahd University of Petroleum and Minerals, Saudi Arabia*

[b] *Imam Abdulrahman Bin Faisal University, Saudi Arabia*

**E-mail: adeoluwaewebajo@gmail.com*

Keywords: alkaline-activated concrete, fresh and hardened properties, morphology and mineralogy, nano-silica, natural Pozzolan, pore structure

Abstract. The effect of admixing nanosilica on the fresh and hardened properties of natural pozzolan (NP) based alkali activated concrete (AAC) was examined. The workability, setting times, engineering properties, durability characteristics and pore structure of concrete were evaluated. In addition, the polymerization mechanism was assessed by SEM and XRD analysis. The results indicated that there was insignificant influence of nanosilica on the flow of mortar, however, the setting times of concrete were prolonged with an increase in the nanosilica content. The prominent phases evolved in XRD pattern were philipsite and anorthite which are form of C/N-A-S-H and C-(A)-S-H gel, respectively. A greater absorption of Al and Ca was observed in the mixes prepared with sizeable amount of nanosilica, which enhanced the microstructure and pore structure characterized by fewer voids (>1000 nm) and more gel pores (<10 nm). It is postulated that both the mechanical properties and durability are beneficially enhanced by the synergistic-interaction of NP-nanosilica.

1. Introduction

Ordinary Portland cement (OPC) manufacturing is an energy intensive process which contributes about 6 % to 8 % of CO_2 emissions of total greenhouse gases (GHGs) [1]. As the cement production is expected to grow steadily to meet the demand coupled with the stringent conditions being imposed by the global community to limit the GHGs emissions, the building materials research has embarked on finding low carbon footprint alternative binders to OPC [2]. Among various options available, alkali activated binder (AAB) has been extensively researched as they are synthesized utilizing industrial by-products as well as natural materials [1, 3–7]. The notable benefits of using AAB are environmental, economic and technical [6, 8, 9]. The technical benefits include high early strength and improved durability, particularly under the exposure of acid and sulfate environments [10–13].

However, the rate of strength development of AABs was found to be slow when cured at room temperature conditions and rapid at elevated temperature curing, particularly those binders synthesized by using low Ca precursor materials [14, 15]. The necessity of curing these binders at elevated temperature is to accelerate the setting in order to achieve sufficient structural strength leading to up-scale the technology to the industrial level. Hence, the synthesis of AABs that can set within the reasonable limits and gain sufficient strength when cured at room temperature conditions would certainly widen its application beyond the precast industry.

With the aim of improving the strength gain of AABs that were synthesized using low Ca precursor materials when cured at lower temperatures, researchers focused on increasing the fineness of the source materials or blending alternative industrial byproducts and natural materials to alter the chemical and

Ibrahim, M., Nasir, M., Hussaini, S.R., Najamuddin, S.K., Ewebajo, A.O. Performance of structurally viable green concrete derived from natural pozzolan and nanosilica. Magazine of Civil Engineering. 2021. 107(7). Article No. 10710. DOI: 10.34910/MCE.107.10

mineralogical composition of the primary source materials [16, 17]. These alternative materials included; metakaolin, silica fume, rise husk ash and blast furnace slag, etc. The alternative materials that contained Ca were found to have greater influence on the fresh and hardened properties of alkali-activated concrete (AAC) [14, 18]. The setting time of AABs that were synthesized using low Ca precursor materials such as low Ca fly ash was delayed, however, inclusion of GGBFS in these mixes accelerated it [19]. This is mainly due to the availability of Ca in the GGBFS which quickly dissolves in water to form a binder. It has been reported that the final setting time of alkali activated low Ca fly ash was more than 24 hours because of slow polymerization at ambient conditions [19].

Whilst, inclusion of OPC in the mixture shortened setting time that was comparable to binder containing OPC alone [19]. Kumar et al. [20] studied the effect of adding 5 to 50 % replacement of fly ash with GGBFS on the reaction kinetics, strength development and microstructure. In another study, Temuujin et al. [16] investigated incorporation of CaO and $Ca(OH)_2$ on the strength development of fly ash based concrete. They observed that Ca enhanced the rate of strength development. De Silva et al. [21] partially replaced GGBFS with metakaolin. Their results revealed that the incorporation of metakaolin delayed the final setting due to delay in the heat release peak. As a result of which there was marginal reduction in the strength as well. The enhanced fresh and hardened properties of AABs that were synthesized using fly ash/GGBFS blends was attributed to the formation of C-S-H along with the polymeric gel such as C/N-A-S-H [22–24].

Recently, nanomaterials have attracted significant interest in the building materials research. The usage of these materials in the cementitious binders has the potential of manipulating the material characteristics at nano-level, thereby enhancing the micro-level properties. It is believed that the finer materials increase the rate of dissolution, consequently, improving the fresh and hardened properties of cementitious binders. The changes in the binder structure at these levels significantly improves the macro-level properties, thus, providing a new functionality to the end product [25, 26]. Several studies were carried out earlier to investigate the use of nanomaterials in the OPC-based binders [27–32].

It was reported that the engineering properties of these binders were enhanced due to the usage of nanomaterials, particularly from nanosilica. It was reported in one of the studies that the compressive strength of mortars prepared with nanosilica was more than that of mortars prepared by incorporating microsilica [27]. The increase in the mechanical strength was attributed to the enhanced pozzolanic reaction in the mixture containing nanosilica. Nazari and Riahi [33] found improvement in the mechanical properties of the concrete due to the addition of nanosilica. They posited that superior properties were attributed to the enhanced formation of C-S-H. They further noticed that the microstructure of binder at 4 % nanosilica addition was dense and uniform compared to the other mixes. The improved properties of nanosilica-based concrete are also due to the fact that it plays vital role in strengthening the interfacial zone between the aggregate and paste [34].

The AABs are formed when the precursor materials are activated in the presence of highly alkaline activators to form polymeric compounds. In the process of poly-condensation, intensive three-dimensional structural network is formed during the formation of AAB. The chain length of the network depends on the reactivity of the source material. Therefore, nanomaterials could possibly play a key role in the case of AAB formation even more than that of OPC-based binders. Firstly, by improving the reactivity of the precursor materials, secondly, by forming stable longer network of three-dimensional polymeric compounds. Taking into account the advantages of nanomaterials, they were also used as partial replacement of fly ash, in the earlier studies with a view to accelerate the polymerization process during the synthesis of AAB. Phoo-ngernkham et al. [35] investigated the usage of nano-silica and nano-alumina on the mechanical and morphological characteristics of fly ash based AAB. Elsewhere, up to 10 % nano-silica was incorporated in the AAB [36]. In their study, 6 % nano-silica was the optimum dosage in yielding improved properties [36].

In an earlier study by authors, synthesis of natural pozzolan as AAB indicated potential in extensive utilization as precursor material in developing viable structural alkali activated concrete [37]. The strength and microstructural properties of NP-based AAC were enhanced by incorporating nanosilica when the binder was cured at room and elevated temperature [38, 39]. Also, the influence of type of alkaline activators on the NP-based concrete was discussed in detail earlier by authors [40]. A detailed study was also reported earlier by authors on the influence of nanosilica on the porosity [41]. Keeping in view the enormous specific surface area of nanomaterials that could possibly enhance the properties of AABs in twofold. Firstly, by improving the polymerization products in the presence of alkaline activators that will decrease the voids in the binder structure. Secondly, by densifying microstructure by particle packing effect which enhances the pore structure of solid and maximizes the gel network. Therefore, this study aims to investigate the effect of nanosilica on the fresh and hardened properties of NP-based AAC focusing on the setting time and pore structure. The results of this study could possibly elucidate the polymerization mechanism of NP-based AAC incorporating nanosilica which would help in characterizing the pore structure and pore size distribution as well.

2. Materials and Methods

2.1. Materials

The oxide composition of natural pozzolan (NP) obtained from X-ray fluoresce (XRF) analysis is depicted in Fig. 1. The physico-chemical properties of nanosilica provided by AkzoNobel supplier are given in Table 1. Na_2SiO_3 (SS) having silica modulus of 3.3 and 14 M NaOH (SH) at a weight ratio of 2.50 was used to activate precursor materials. The granulometry of coarse aggregate (CA) used was conforming to ASTM C33 curve #8 [42] wherein 60 % of 4.75 mm, 35 % of 2.36 mm and 5 % of 1.18 mm size of aggregates were proportioned. The particle size distribution of the fine aggregates (FA) are summarized in Table 2.

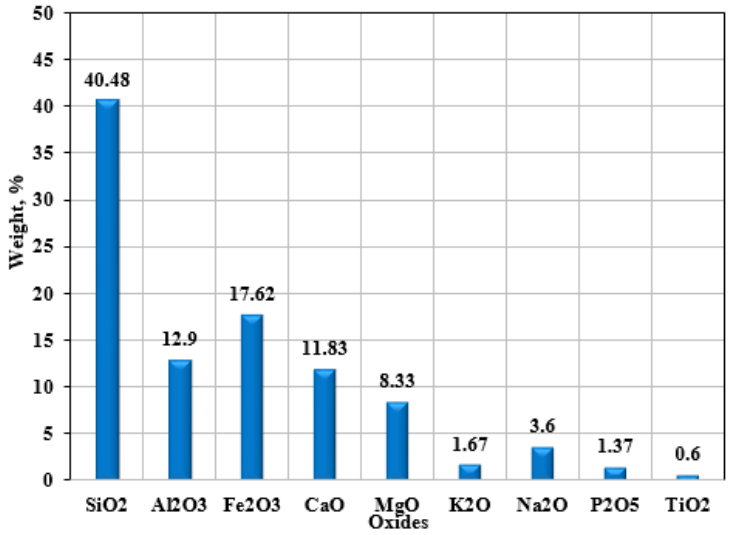

Figure 1. Oxide composition of NP by XRF.

Table 1. Physico-chemical properties of nanosilica.

Parameters	Properties
SiO_2	99 %
Al_20_3	1.20 %
TiO_2	0.03 %
Fe_20_3	0.01 %
pH-value	9.5
Mean Particle size	35 nm
Surface area	80 m^2/g
Solid matter content	50 %
Density	1.2–1.4 g/cm^3

Table 2. Particle size distribution of fine aggregate.

ASTM Sieve #	Size	% passing
4	4.75 mm	100
8	2.36 mm	100
16	1.18 mm	100
30	600 µm	76
50	300 µm	10
100	150 µm	4

2.2. Methods

2.2.1. Mix composition and curing

A set of five alkali-activated natural pozzolan-based mixtures were cast by admixing 0 %, 1 %, 2.5 %, 5% and 7.5 % of nanosilica. The following parameters were kept invariant: total binder content was 400 kg/m^3, SS was 150 kg/m^3, SH was 60 kg/m^3, while FA and CA was approximately 635 kg/m^3 and 1179 kg/m^3, respectively [41]. Besides, a conventional concrete mix was also prepared having 370 kg/m^3 of binder and

water to cement ratio of 0.45 in order to compare with AAC. AAC samples for each mix were prepared by firstly making liquid portion of the mixture by adding required quantities of SS, SH and colloidal nanosilica followed by sonication to disperse it properly. Subsequently, dry materials were introduced in the Hobart paddle mixer and mixed thoroughly. Afterwards, the alkaline solution was mixed until the substance became homogeneous. Next, the fresh concrete was filled in to the moulds in two segments and demolded after 24 hours. All the prepared specimens were cured at the ambient laboratory condition (Temp: 23±2 °C and RH 50±5 %) until testing.

2.2.2. Fresh properties

The workability was determined by conducting flow table test according to ASTM C1437 [43]. The setting times of concrete were determined by measuring penetration resistance in accordance with ASTM C403 [44].

2.2.3. Hardened properties

NMR relaxometry using a GeoSpec 2–75 core analyzer was used to study the pore structure of concrete. The cylindrical specimens of size 40 mm diameter and 40 mm height were utilized. Prior to the test, specimens were fully saturated under 10 MPa pressure [45, 46]. The compressive strength, flexural strength and modulus of elasticity of concrete were determined according to ASTM C109 [47], C78 [48] and C469 [49] respectively.

The water absorption and volume of permeable voids (VPV) were measured utilizing Ø75 mm × 150 mm high cylindrical specimens according to the procedure described in ASTM C642 [50]. Most importantly, modified rapid chloride permeability and non-steady state chloride migration coefficient were also determined in accordance with the procedure outlined by Noushini and Castel [8] and NT Build 492 [51] respectively, for all the AAC mixes along with the conventional concrete. The measurements were conducted post 28 and 90 days of ambient temperature curing.

3. Results and Discussion

3.1. Influence of nanosilica on the fresh properties of binder

The plots of penetration resistance versus elapsed time for various concrete mixes is shown in Fig. 2(a) to 2(f). For each plot, a befitting exponential curve was drawn and equation was obtained. Subsequently, the initial setting time and final setting time were computed by taking 3.5 MPa and 27.6 MPa as the penetration resistance, respectively. The alkaline activator, a liquid portion in the mixture, is the essential component in the synthesis of AABs. According to the methodology presented elsewhere to perform setting times test [52], ASTM C191 [53] was followed in which normal consistency was determined by adjusting alkaline activator content in the mixture. However, adjusting alkaline activator content in order to achieve normal consistency of the AAB in accordance with ASTM C191 [53] has been originally specified for OPC based binder, may not be appropriate to be used for AABs. This concern was also expressed by Teixeira-Pinto et al. [54]. This is particularly true because of the fact that the chemical ingredients present in the alkaline activator participate in the chemical reaction in which precursor material is transformed in to a polymeric compound such as C-A-S-H or N-A-S-H or both depending on the composition of the source materials [55, 56].

Hence, determining the setting times of AABs by utilizing concrete in accordance with ASTM C403 [44] which does not require liquid portion to be adjusted is more appropriate. It is also worth mentioning that the initial and final setting times of any binder are essentially required to plan the concreting work. Duration of initial setting is of importance that determines when the concrete is no longer be workable and prior to which consolidation and finishing works could be scheduled. Similarly, determining the final setting time of concrete is also important to know when the concrete can start to take the loads.

Table 3 summarizes the initial and final setting times of the AAC incorporating nanosilica along with the OPC based concrete. As expected, the initial and final setting times of the OPC based concrete were less compared to the AAC containing variable quantity of nanosilica. The average initial setting time was in the range of 4 h 52 min to 6 h 37 min, while, the final setting time was between 6 h 50 min and 9 h 9 min. As mentioned earlier, the penetration resistance test was conducted in the laboratory conditions (at 23±2 °C and 50±5 % RH). The quantity of lime (CaO) in the source material accelerates the setting of AAB as it dissolves relatively quickly compared to Si and Al [57]. Nath and Sarker [19] studied the effect of adding GGBFS on the fly ash based AAB cured in ambient conditions discovered that the GGBFS content accelerated the setting of binder. According to their results the setting of AAB prepared without GGBFS was more than 24 hours, while, 10 % addition resulted in initial and final setting times of 290 min and 540 min, respectively. The initial and final setting times of AAC synthesized without nanosilica in this study was on average 4 h 52 min and 6 h 50 min, respectively. Both the setting times were prolonged in the AAC mixtures as the NP replacement with nanosilica was increased. Similar results were observed in the previous research conducted by Gao et al. [58].

As reported in a previous study that the first step in the process of alkali activation is the dissolution of source material in to the highly alkaline solution [59]. When nanosilica is added in the mixture, due to an increase in the concentration of Si, pH of the alkaline solution drops which delays the reaction. This was also proven by the calorimetric studies carried out by Deir et al. [57] wherein high silica content delayed the heat release peak. This phenomenon has delayed the setting of NP-based binder modified with nanosilica. Another important factor which retarded the setting was the reduction in CaO content in the mixture when nanosilica was added as a replacement of NP (Fig. 1). Though the nanosilica dissolves quickly in the alkaline solution, this effectively retards the dissolution of Si and Al of the precursor material unless the high alkalinity breaks the layers to dissolve these species from the source material (Fig. 1 and Table 1). Thus, the combined influence of these factors played a role in delaying the setting times of NP-based AAC modified with nanosilica. However, the overall setting times of the AAC containing nanosilica were reasonable to be used in cast in place applications.

Table 4 shows the flow of alkali activated mortar. There was marginal increase in the flow of mortar as the quantity of nanosilica increased in the mix up to a replacement level of 2.5 %. Beyond this replacement level, the workability was slightly reduced. Apparently, there was no adverse influence on the workability of binder due to the addition of nanosilica. At higher replacement levels, decrease in the flow of mortar could be attributed to the increase in water demand because of increase in specific surface area of nano particles (Table 1). Since the flow of mortar was between the range of 140 to 200 mm in all mixture, they are characterized as plastic flow as recently reported by [18].

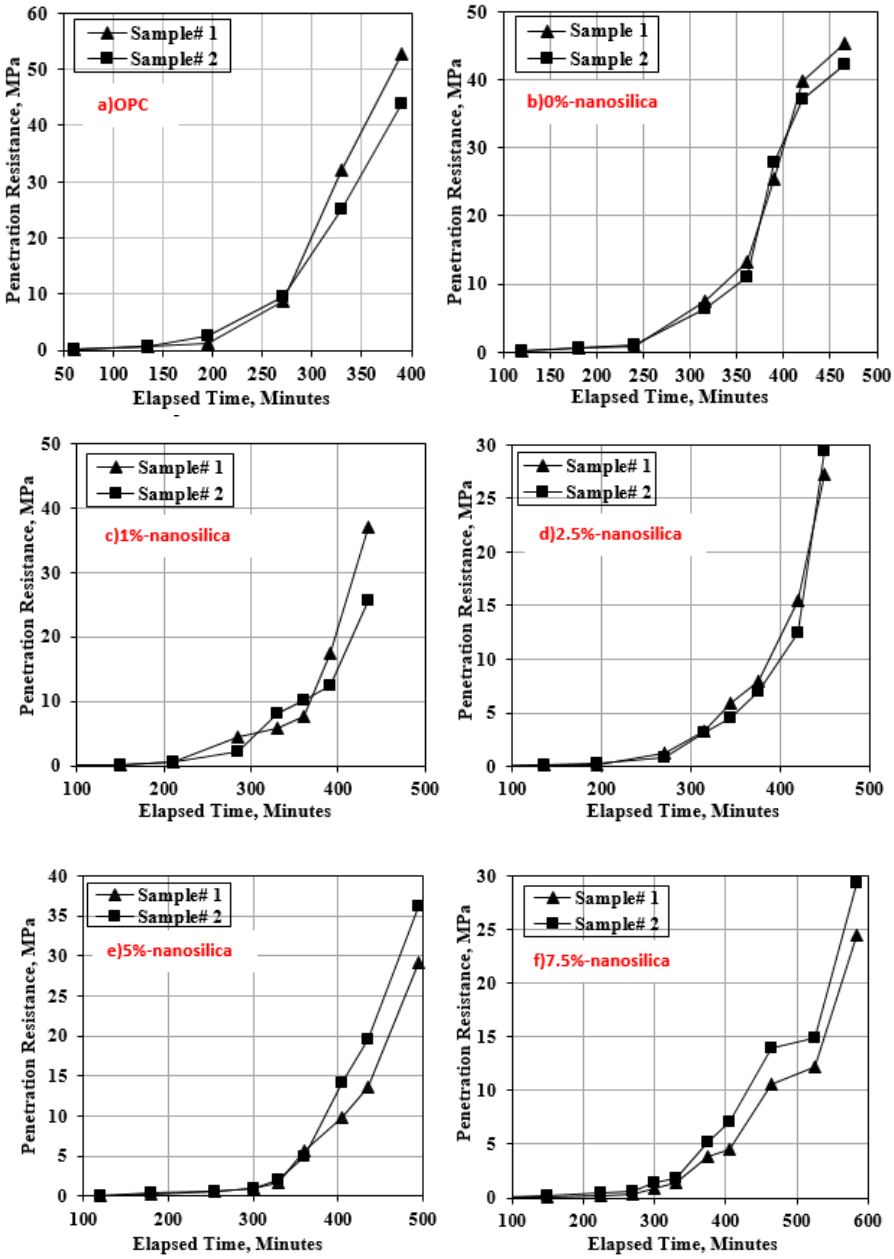

Figure 2(a-f). Penetration resistance versus elapsed time of concrete.

Table 3. Setting times of various concrete mixes.

Mix #	Sample 1		Sample 2	
	Initial setting time, min	Final setting time, min	Initial setting time, min	Final setting time, min
OPC	3 h 56 min	5 h 38 min	3 h 54 min	5 h 39 min
0 %-nanosilica	4 h 48 min	6 h 48 min	4 h 56 min	6 h 52 min
1 %-nanosilica	5 h 6 min	6 h 47 min	5 h 11 min	6 h 59 min
2.5 %-nanosilica	5 h 31 min	7 h 24 min	5 h 38 min	7 h 19 min
5 %-nanosilica	5 h 56 min	7 h 56 min	5 h 42 min	7 h 58 min
7.5 %-nanosilica	6 h 52 min	9 h 14 min	6 h 22 min	9 h 5 min

Table 4. Flow of nanosilica incorporated mortar.

Mix #	Flow of mortar, mm				
	1	2	3	4	Average
0 %-nanosilica	162	166	169	160	164
1 %-nanosilica	174	167	175	165	170
2.5 %-nanosilica	175	168	172	173	172
5 %-nanosilica	162	159	155	155	158
7.5 %-nanosilica	147	155	154	152	152

3.2. Influence of nanosilica on the hardened properties of binder

The pore structure and pore size distribution of hardened cementitious materials govern the micro- and macro-level properties of concrete. By and large the pores in the hardened cementitious materials are categorized into four types depending on the pore diameter. These are: (1) gel pores, (2) small capillary pores, (3) large capillary pores and (4) voids, respectively, having a pore diameter <10, 10 to 100, 100 to 1000 and >1000 nm [60]. The incremental porosity data obtained through the NMR relaxometry was used to calculate contributive porosity of the concrete specimens. The contributive porosity is defined as the proportion of certain category of pores with respect to the total pore volume of the solid. The contributive porosity of various concrete mixes is shown in the Fig. 3 and Fig. 4 that were cured for 28 and 90 days, respectively. The following observations were made:

- Predominantly, the pore diameter was between 1 nm and 100 μm in the various concrete mixes.
- After 28-day curing, the percentage of gel pores (diameter **<**10 nm) was 1.13 % in the control AAC mixture, while, they were between 2.59 % and 2.85 % in the mixes containing nanosilica.
- However, the pores having diameter >10 nm were in greater proportion in the AAC mix prepared with 0 % nanosilica in relation to the mixes having 1 to 7.5 % nanosilica.
- The extent of pores having diameter between 100 and 1000 nm were about 4 % in the 0 % nanosilica at 28 days, whereas 1.85, 1.98, 1.44 and 1.40 % in 1, 2.5, 5 and 7.5 % nanosilica, respectively.
- Further, highest of about 7 % of pores having diameter more than 1000 nm were obtained in the 0 % nanosilica, while 4.73, 5.76, 4.33, and 3.95 % in the 1, 2.5, 5 and 7.5 % nanosilica, respectively.
- The continuation of curing from 28 to 90 days, marginally reduced the gel pores (<10 nm) in all the concrete mixes, however, there was significant reduction in the volume of pores classified as voids (>1000 nm). This was particularly noticeable in the mixes prepared with increased nanosilica content.
- Besides, the percentage of pores having diameter <10 nm increased with the nanosilica quantity increment in the mix. The quantity of these pores was twice in the nanosilica modified concrete compared to the control mix at 28 days. Regardless of curing period, the range of pores having diameter in the range of 100 to 1000 nm together with >1000 nm was proportionately reduced with an increase in nanosilica content in the mixture.

Therefore, incorporation of nanosilica in the mixture resulted in higher volume of gel pores and lower voids. The total pore volume was in the range of 11.23 % to 18.35 % such that lowest was recorded in the 7.5 % nanosilica modified concrete and the highest in the reference AAC batch (Table 6). The results obtained in this research are in good agreement with results of a study by Rodríguez et al. [61], wherein an overall porosity was in the range of 6.32 % to 9.75 %. Similar trend was also noted elsewhere [62]. Shaikh et al. [63] adduced that nanosilica forms an envelope to the aggregates consequently lowering capillary pores in the

adjacent matrix. A detailed discussion about the pore structure has been reported in a recent publication of the authors [41].

The refinement of the pore structure in the case of binder prepared with nanosilica is possibly due to the enhanced polycondensation of alkaline-activated products. Evidently, as shown in the Fig. 5(a) to 5(e), the morphology of the binder tends to densify with an increase in nanosilica content in the alkali activated concrete mix. The micrograph of AAB prepared without nanosilica was relatively inhomogeneous, as shown in the Fig. 5(a). It appears to be composed of a non-uniform structure. Due to the termination of polymerization there was insufficient gel formation observed. Fig. 5(b) through 5(e) shows the micrographs of nanosilica incorporated mixes. Evidently, the matrix enhanced as the quantity of nanosilica is increased. The effect of nanosilica on the microstructure of NP-based binder has been discussed in detail in a previously published work elsewhere [39].

The products formed due to alkaline-activation included a philipsite phase that was most prominent in the XRD patterns, as shown in the Fig. 6. It is a form of C-A-S-H gel having Na in the framework [64]. Also, anorthite was detected in the XRD pattern whose structure resembles with C-A-S-H gel without Na in the framework [64]. In addition, the phases such as, C-S-H, quartz, hematite, calcite, and zeolite-Y also appeared in the spectra. These are the phases which determine the nature of the binder and are responsible for imparting skeletal strength. The crystallinity of these phases governs the physical properties of these binders. A close observation at the different XRD patterns reveals that the philipsite, anorthite, C-A-S-H and zeolite-Y peaks were sharp and wide in the case of AAB containing higher nanosilica. Mainly, the philipsite peak around 32.7° and 52° 2θ is seemingly intense and wider in the case of AAB prepared with 5 % and 7.5 % nanosilica. In addition, the concentration of the peak at 36° 2θ associated to C-A-S-H gel was strong in the case of AAB prepared with more than 2.5 % nanosilica.

The primary difference between the hydration products of OPC and AAB is that, C-S-H is formed in the case of former, while in the latter either Al or Na or both are absorbed in the C-S-H to form C-A-S-H or C/N-A-S-H [65]. It is an important gel product formed in the polymerization mechanism of AAB which is believed to be denser than that of C-S-H [65]. Due to the enormous specific surface area of nanosilica particles, reactivity may have been enhanced that promoted the polycondensation process of supplementary C-A-S-H phase in the binder structure [66, 67]. This is particularly true due to the fact that the ratio of Al/Si was high in the AAB synthesized with sizeable quantity of nanosilica according to energy dispersive spectroscopy (EDS) data discussed in detail by the authors [39].

As a result of enhanced polycondensation due to superior formation of hydration products, the mechanical properties of the AAC prepared with partially replacing NP with nanosilica were significantly improved. Table 5 summarizes compressive and flexural strength along with the modulus of elasticity of AAC.

The compressive strength of concrete was lower at 7 days in the AAC incorporating nanosilica. The greater quantity of nano-silica retarded strength development. On contrary, at later ages after 28 and 90 days, there was significant development in compressive strength noted in the 5 as well as 7.5 % nanosilica incorporated binder. However, slow strength gain in the AAC modified with 7.5 % nanosilica was noted which may possibly be attributed to embedded remnants of unreacted particles in the binder structure observed in the micrograph (Fig. 5). Also, the addition of higher quantity of silica believed to delay the heat release peak as a result of decrease in the pH [57]. It is important to indicate here that the strength gain in the nanosilica modified concrete was rather slow owing to the slow cross-linking of polymeric units [68].

It is demonstrated that the cross-linking takes place faster when the AABs are cured at elevated temperature [68]. However, curing these binders at elevated temperature could possibly solidify the gel prematurely which will discontinue the dissolution of aluminates and silicates of the precursor material in to the alkaline solution. Thereby, terminating the process of polymerization which hampers the formation of polymeric units [69, 70]. This connotes that admixing nanosilica involves slow reaction kinetics at early ages, whereas admixing more than 5 % of nanosilica negatively affects the long-term strength development.

Mixes prepared with admixing more than 2.5 % nanosilica also gained superior flexural strength. Though there was high early strength in the OPC-based concrete, it was about 60 % lower when compared with the 5 % and 7.5 % nanosilica added AAC cured for 90 days. The flexural strength of AAC incorporating nanosilica was superior to OPC-based concrete. It is to be noted that the elastic modulus of AAC of similar grades is lower compared to the conventional concrete (Table 5). The influence of nanosilica is clearly evident from the mechanical properties of AAC and an increase in the nano particles in the binder structure improved compressive strength, flexural strength and modulus of elasticity which corroborates the findings of total porosity, as demonstrated in Table 6. The total porosity was more or less proportional to the nanosilica content in the batch.

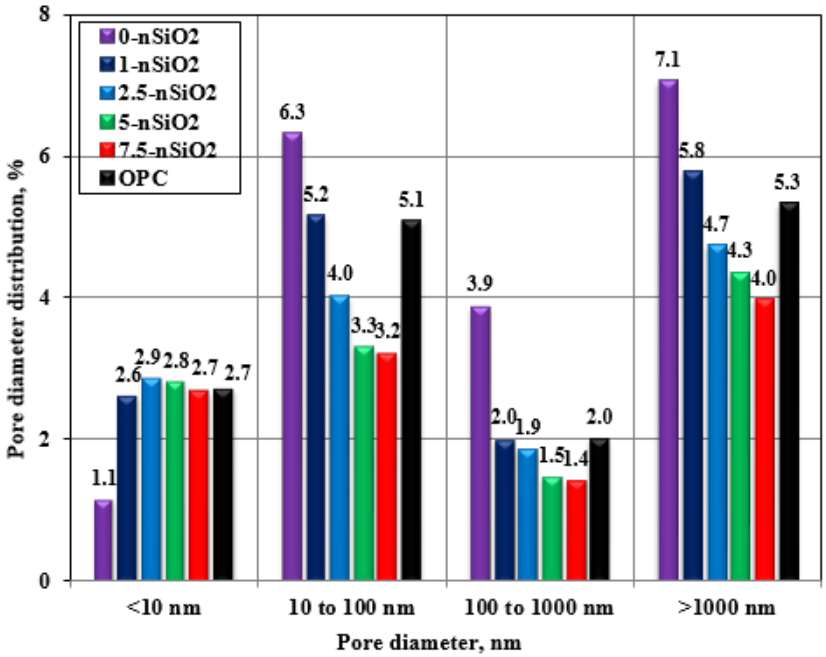

Figure 3. Contributive porosity of concrete after 28 days of curing.

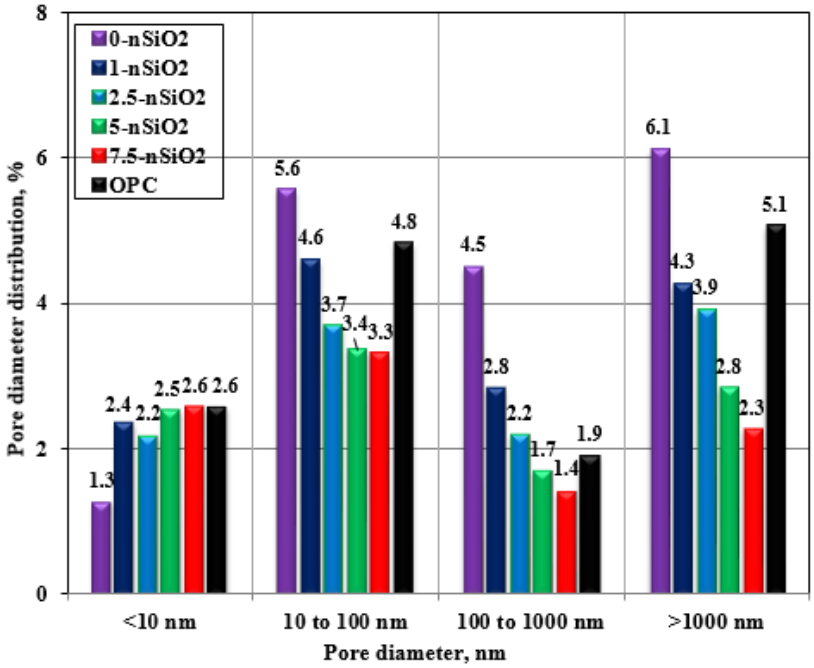

Figure 4. Contributive porosity of concrete after 90 days of curing.

Table 6. Cumulative pore volume in the concrete.

Mix #	Cumulative pore volume, %	
	28-days	90-days
OPC	15.05	14.34
0 %-nanosilica	18.35	17.43
1 %-nanosilica	15.49	14.03
2.5 %-nanosilica	13.45	11.92
5 %-nanosilica	11.86	10.39
7.5 %-nanosilica	11.23	9.53

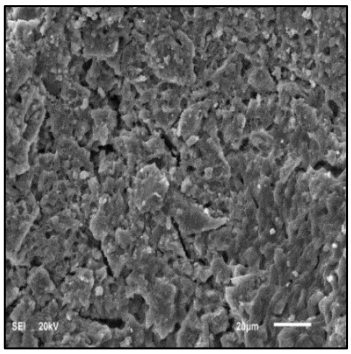

(a) 0 %-nanosilica

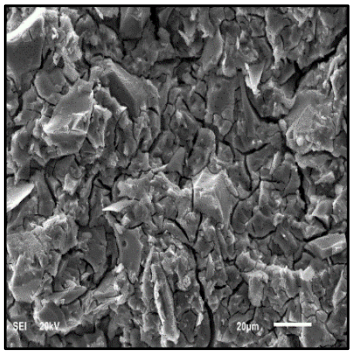

(b) 1 %-nanosilica

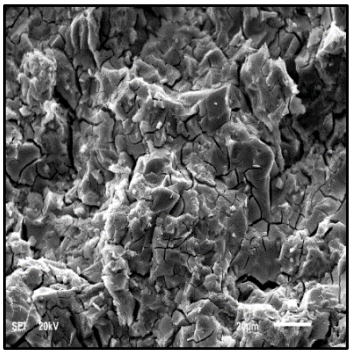

(c) 2.5 %-nanosilica

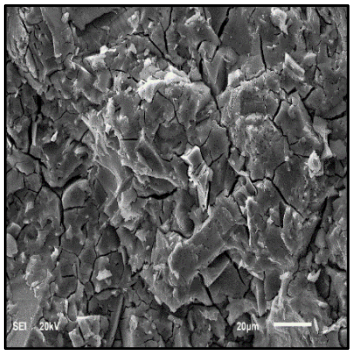

(d) 5 %-nanosilica

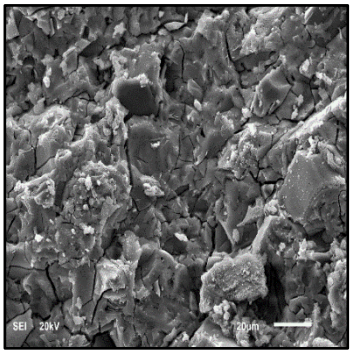

(e) 7.5 %-nanosilica

Figure 5(a-e). Micrographs of AAC incorporating nanosilica.

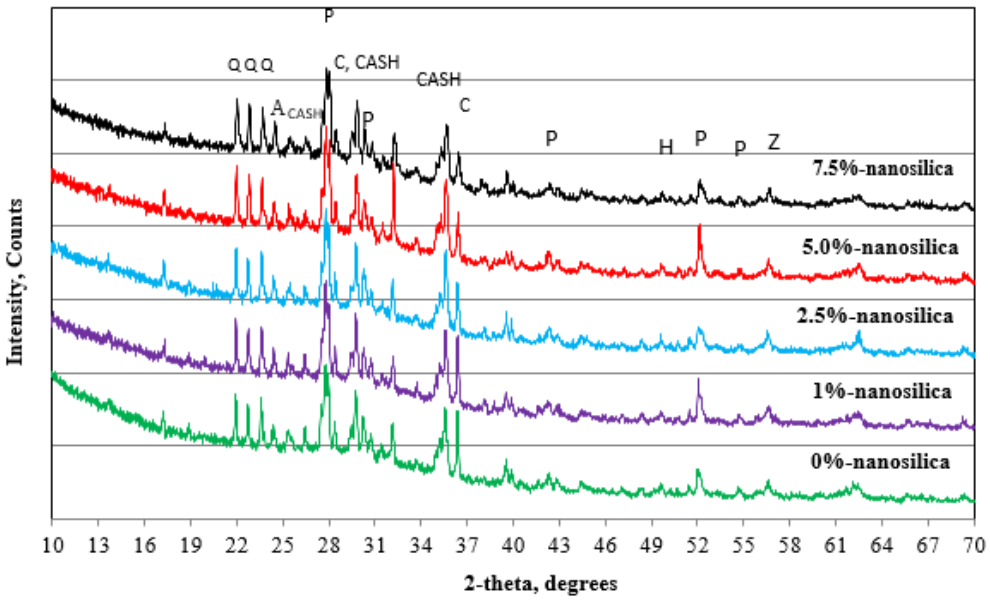

Figure 6. XRD of different AABs incorporating nanosilica. (Q:Quartz, CASH: Calcium Alumina Silicate Hydrate, P; Philipsite, C: Calcite, Z; Zeolite Y, A; Aluminosilicate, H; Hematite).

Table 5. Mechanical properties of various AAC mixes.

	Compressive strength, MPa			Flexural strength, MPa		Modulus of Elasticity, GPa	
Mix #	7d	28d	90d	28d	90d	28d	90d
OPC	24.3	35.5	36.3	4.5	4.6	24.4	25.1
0 %-nanosilica	13.8	25.5	27.9	3.9	4.9	13.8	14.5
1 %-nanosilica	14.2	28.4	31.4	4.2	5.1	15.2	15.9
2.5 %-nanosilica	11.6	29.8	36.3	4.9	5.5	16.0	18.1
5 %-nanosilica	9.4	45.0	60.6	6.2	7.5	24.0	28.7
7.5 %-nanosilica	7.8	38.0	58.8	6.1	7.6	19.4	27.0

3.3. Influence of nanosilica on the durability of concrete

The water absorption and volume of permeable voids are among the very important durability characteristics of the hardened concrete. Water absorption in the range of 3 % to 6 % is generally categorized as good concrete suitable for structural applications. The water absorption of hardened AAC prepared by combination of NP and nanosilica after 28 and 90 days of room curing is shown in Fig. 7. It decreased as the nanosilica content increased in the mix. It was in the range of 4.20 % to 5.89 % and 3.52 % to 5.15 % after 28 days and 90 days of curing, respectively. As expected, the water absorption reduced when the curing progressed from 28 days to 90 days. The maximum value of 5.12 % was recorded in the AAC mixture prepared without nanosilica, while it was about 4.85 %, 4.82 %, 3.52 % and 3.45 %, respectively, in the concrete mixes containing 1 %, 2.5 %, 5 % and 7.5 % nanosilica after 90 days of room temperature curing.

The results of volume of permeable voids are shown in Fig. 8 which appears to be following similar trend as water absorption. The volume of permeable voids tended to lower linearly with an increase in nanosilica content. The water absorption and volume of permeable voids in the OPC based concrete was more or less similar to the results obtained for the AAC prepared with lower level of nanosilica. However, the percentage of water absorption and volume of permeable voids of the AAC prepared with 5 % and 7.5 % nanosilica was considerably lower than that of the OPC concrete as well as the control alkali activated mix.

The results support the notion developed in SEM analysis (Fig 5) wherein enhancement in the microstructure was evident owing to the refinement in the pore structure attributed to the greater enrichment and intertwining of the polymeric compound in the nanosilica modified concrete (Fig. 6). These trends were reflected on the chloride permeability and migration coefficient data. There was reduction in the chloride permeability and the coefficient of chloride migration with an increase in nanosilica content, as summarized in Table 7. The chloride permeability was between 343 and 579 Coulombs in the various AAC mixes after 28 days of ambient curing, which obviously reduced with the continuation of curing up to 90 days. The lowest permeability was observed in the AAC prepared with highest nanosilica content. Similar trend was observed in the case of chloride migration coefficient. It was in the range of 6.93 to 16.68 ($\times 10^{-12}$) m^2/s in the AAC after 28 days of curing, lowest in the 7.5 % nanosilica and highest in the control AAC mix.

However, the chloride permeability was lower in the OPC concrete compared to any AAC mix investigated in this study. Nonetheless, the chloride migration coefficient in the conventional OPC concrete was comparable to the 2.5 % nanosilica mixture. When the chloride permeability was carried out using 60V potential based on ASTM C1202, the charge passed was estimated to be about 8250 Coulombs in the fly ash based AAC reported by Thomas et al. [71]. The authors have expressed concern about the heat generation in the chloride permeability cell. However, inclusion of GGBFS in the binder improved the results. A free chloride diffusion coefficient in the fly ash based binder was more than 38 ($\times 10^{-12}$) m^2/s, while between 6 and 8 ($\times 10^{-12}$) m^2/s was measured in the GGBFS modifiend concrete [71]. A study conducted by Ravikumar and Neithalath [72] reported a chloride migration coefficient of about 7 ($\times 10^{-12}$) m^2/s for a GGBFS content of 400 kg/m^3 activated with an alkaline activator having silica modulus of 1.5. Hence, the results obtained in this study are in compliance to the results reported in the earlier studies.

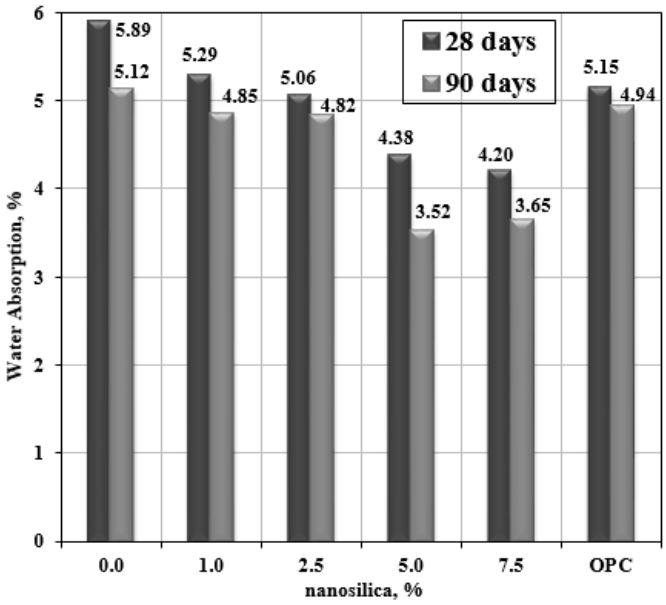

Figure 7. Water absorption of concrete.

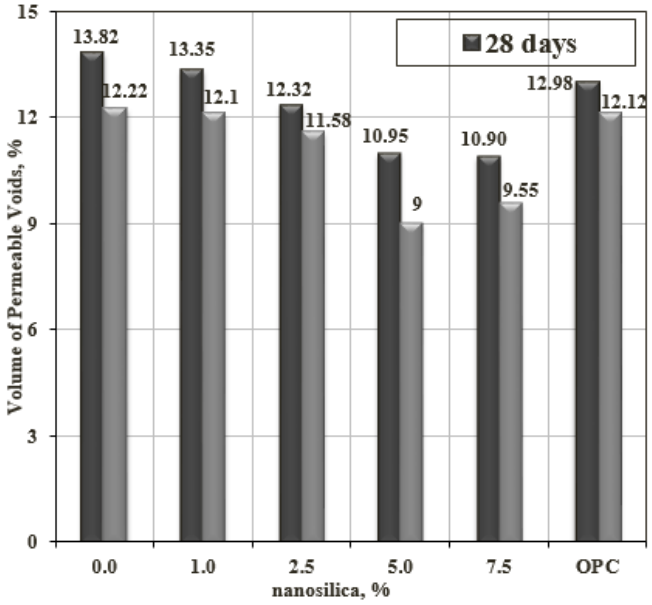

Figure 8. Volume of permeable voids of concrete.

Table 7. Chloride permeability and migration coefficients in the AAC.

Mix #	Chloride permeability, Coulombs		Chloride migration coefficient, m^2/s ($\times 10^{-12}$)	
	28d	90d	28d	90d
OPC	337	323	12.43	10.44
0 %-nanosilica	579	551	16.68	12.83
1 %-nanosilica	549	527	14.67	12.63
2.5 %-nanosilica	479	456	11.74	10.52
5 %-nanosilica	348	327	8.70	7.83
7.5 %-nanosilica	343	322	6.93	6.22

4. Conclusions

The objective of this study was to evaluate the fresh and hardened properties of natural pozzolan (NP)-based alkali activated concrete (AAC) synthesized at low temperature curing. The effect of nanosilica was studied by substituting varying nanosilica dosages up to 7.5 %. Following conclusions could be drawn:

- There was positive impact of admixing up to 2.5 % of nanosilica on the workability due to lubricating effect provided by nanosilica and thereafter the mix tend to stiffen.
- The setting times were retarded with increment in nanosilica content ascribed to the slow dissolution of Si and Al from the precursor material as well as reduction in CaO content present in NP.
- The incorporation of nanosilica significantly improved the microstructure which consequently refined the pore structure by reducing voids and increasing the gel pores. There was increased absorption of Ca and Al attributed to enhancement in the polycondensation process. The formation of philipsite whose structure is similar to C/N-A-S-H contributed to strength skeleton.
- It is postulated that the synergism of NP and up to 5 % of nanosilica significantly improves the mechanical properties, whereas up to 7.5 % nanosilica is beneficial for enhancing the durability characteristics due to both chemical as well as physical influence on the binder structure.

It is envisioned that the effect of other nano materials, such as nano-alumina in improving the pore structure of NP-based AAB may also be interesting and further add value to the literature.

5. Acknowledgment

The authors gratefully acknowledge the Center for Engineering Research (CER) of the Research Institute and Center for Integrative Petroleum Research, King Fahd University of Petroleum and Minerals, Dhahran, Saudi Arabia.

References

1. Ankur, M., Rafat, S. An overview of geopolymers derived from industrial by-products. Constr. Build. Mater. 2016. 127. Pp. 183–198.
2. Galishnikova, V.V., Abdo, Sh., Fawzy, A.M. Influence of silica fume on the pervious concrete with different levels of recycled aggregates. Magazine of Civil Engineering. 2020. 93(1). Pp. 71–82. DOI: 10.18720/MCE.93.7
3. Ryu, G.S., Lee, Y.B., Koh, K.T., Chung, Y.S. The mechanical properties of fly ashbased geopolymer concrete with alkaline activators, Constr. Build. Mater. 2013. 47. Pp. 409–418.
4. Davidovits, J. Geopolymer chemistry and sustainable development – the poly(sialate) terminology: a very useful and simple model for the promotion and understanding of green-chemistry, in: J. Davidovits (Ed.), Proceedings of the World Congress Geopolymer, Saint Quentin, France, 2005. 69–73.
5. Adewumi, A.A., Ismail, M., Ariffin, M.A.M., Yusuf, M.O., Maslehuddin, M., Mohamed, H.D. Strength and microstructure of alkali-activated natural pozzolan and limestone powder mortar. Magazine of Civil Engineering. 2019. 92(8). Pp. 36–47. DOI: 10.18720/MCE.92.3
6. Yusuf, M.O., Megat Johari, M.A., Ahmad, Z.A., Maslehuddin, M. Strength and microstructure of alkali-activated binary blended binder containing palm oil fuel ash and ground blast-furnace slag. Construction and Building Materials. 2014. 52. Pp. 504–510.
7. Sharonova, O.M., Yumashev, V.V., Solovyov, L.A., Anshits, A.G. The fine high-calcium fly ash as the basis of composite cementing material. Magazine of Civil Engineering. 2019. 91(7). Pp. 60–72. DOI: 10.18720/MCE.91.6
8. Noushini, A., Castel, A. Performance-based criteria to assess the suitability of geopolymer concrete in marine environments using modified ASTM C1202 and ASTM C1556 methods. Materials and Structures. 2018. 51(146). Pp. 1–16.
9. Dvorkin, L.I. The Influence of Polyfunctional Modifier Additives on Properties of Cement-Ash Fine-Grained Concrete. Magazine of Civil Engineering. 2020. 93(1). Pp. 121–133. DOI: 10.18720/MCE.93.10
10. Tayeh, B.A., Al Saffar, D.M., Aadi, A.S., Almeshal, I. Sulphate resistance of cement mortar contains glass powder. Journal of King Saud University: Engineering Sciences. 2019.
11. Tayeh, B.A., Hasaniyah, M.W., Zeyad, A.M., Awad, M.M., Alaskar, A., Mohamed, A.M., Alyousef, R. Durability and mechanical properties of seashell partially-replaced cement. Journal of Building Engineering. 2020. 101328.
12. Nasir, M., Megat Johari, M.A., Maslehuddin, M., Yusuf, M.O. Sulfuric acid resistance of alkali/slag activated silico-manganese fume-based mortars. Structural Concrete. 2020. 2020b. Pp. 1–15. DOI: 10.1002/suco.201900543
13. Nasir, M., Megat Johari, M.A., Maslehuddin, M., Yusuf, M.O. Sulfuric acid resistance of alkali/slag activated silico-manganese fume-based mortars. Structural Concrete. 2020. 2020c. Pp. 1–15. DOI: 10.1002/suco.202000079
14. Nasir, M., Johari, M.A.M., Yusuf, M.O., Maslehuddin, M., Al-Harthi, M.A., Dafalla, H. Impact of Slag Content and Curing Methods on the Strength of Alkaline-Activated Silico-Manganese Fume/Blast Furnace Slag Mortars. Arabian Journal for Science and Engineering. 2019. 44(10). Pp. 8325–8335.
15. Nasir, M., Johari, M.A.M., Maslehuddin, M., Yusuf, M.O., Al-Harthi, M.A. Influence of heat curing period and temperature on the strength of silico-manganese fume-blast furnace slag-based alkali-activated mortar. Construction and Building Materials. 2020. 251. 118961.
16. Temuujin, J., Williams, R., van Riessen, A. Effect of mechanical activation of fly ash on the properties of geopolymer cured at ambient temperature. Journal of Materials Processing Technology. 2009. 209(12-13). Pp. 5276–5280. DOI: 10.1016/j.jmatprotec.2009.03.016

17. Somna, K., Jaturapitakkul, C., Kajitvichyanukul, P., Chindaprasirt, P. NaOH activated ground fly ash geopolymer cured at ambient temperature. Fuel. 2011. 90(6). 21182124. DOI: 10.1016/j.fuel.2011.01.018
18. Nasir, M., Johari, M.A.M., Yusuf, M.O., Maslehuddin, M., Al-Harthi, M.A. Synthesis of Alkali-Activated Binary Blended Silico-Manganese Fume and Ground Blast Furnace Slag Mortar. Journal of Advanced Concrete Technology. 2019. 17(12). Pp. 728–735.
19. Nath, P., Sarker, P.K. Effect of GGBFS on setting, workability and early strength properties of fly ash geopolymer concrete cured in ambient condition. Construction and Building Materials. 2014. 66. Pp. 163–171.
20. Kumar, S., Kumar, R., Mehrotra, S.P. Influence of granulated blast furnace slag on the reaction, structure and properties of fly ash based geopolymer. Journal of Materials Science. 2010. 45(3). Pp. 607–615. DOI: 10.1007/s10853-009-3934-5
21. De Silva, P., Sagoe-Crenstil, K., Sirivivatnanon, V. Kinetics of geopolymerization: Role of Al_2O_3 and SiO_2. Cement and Concrete Research. 2007. 37(4). Pp. 512–518. DOI: 10.1016/j.cemconres.2007.01.003
22. Granizo, M.L., Alonso, S., Blanco-Varela, M.T., Palomo, A. Alkaline Activation of Metakaolin: Effect of Calcium Hydroxide in the Products of Reaction. Journal of the American Ceramic Society. 2002. 85(1). Pp. 225–231. DOI: 10.1111/j.1151-2916.2002.tb00070.x
23. Dombrowski, K., Buchwald, A., Weil, M. The influence of calcium content on the structure and thermal performance of fly ash based geopolymers. Journal of Materials Science. 2007. 42(9). Pp. 3033–3043. DOI: 10.1007/s10853-006-0532-7
24. Yip, C.K., Lukey, G.C., Provis, J.L., van Deventer, J.S.J. Effect of calcium silicate sources on geopolymerisation. Cement and Concrete Research. 2008. 38(4). Pp. 554–564. DOI: 10.1016/j.cemconres.2007.11.001
25. Jayapalan, A.R., Lee, B.Y., Kurtis, K.E. Can nanotechnology be 'green'? Comparing efficacy of nano and microparticles in cementitious materials. Cement and Concrete Composites. 2013. 36. Pp. 16–24.
26. Balaguru, P., Chong, K. Nanotechnology and Concrete: Research Opportunities. Proceedings of ACI Session on Nanotechno-logy of Concrete: Recent Developments and Future Perspectives. Denver, USA, Nov. 7, 2006.
27. Jo, B., Park, J., Tae, G., Kim, C. Characteristics of cement mortar with nano-SiO_2 particles. Construction and Building Materials. 2007. 21. Pp. 1351–1355.
28. Ozyildirim, C., Zegetosky, C. Exploratory Investigation of Nanomaterials to Improve Strength and Permeability of Concrete. Journal of the Transportation Research Board. 2010. Pp. 1–8.
29. Hosseini, P., Booshehrian, A., Farshchi, S. Influence of Nano-SiO_2 Addition on Microstructure and Mechanical Properties of Cement Mortars for Ferrocement, Journal of the Transportation Research Board. 2010. Pp. 15–20.
30. Belkowitz, J.S. An Investigation of Nano Silica in the Cement Hydration Process. MSc thesis. University of Denver, 2009.
31. Amiri, B., Bahari, A., Nik, A.S., Movahedi, N.S. Use of AFM technique to study the nanosilica effects in concrete mixture. Indian Journal of Science and Technology. 2012. 5(2). Pp. 2055–2059.
32. Polat, R., Demirboğa, R., Karagöl, F. Mechanical and physical behavior of cement paste and mortar incorporating nano-CaO. Structural Concrete. 2019. 20(1). Pp. 361–370.
33. Nazari, A., Riahi, S. Microstructural, thermal, physical and mechanical behavior of the self-compacting concrete containing SiO2 nanoparticles. Materials Science and Engineering A. 2010. 527. Pp. 7663–7672.
34. Qing, Y., Zenan, Z., Deyu, K., Rongshen, C. Influence of nano-SiO_2 addition on properties of hardened cement paste as compared with silica fume. Construction and Building Materials. 2007. 21. Pp. 539–545.
35. Phoo-Ngernkham, T., Chindraprasirt, P., Sata, V., Hanjitsuwan, S., Hatanaka, S. The effect of adding nanosilica and nano-Al_2O_3 on properties of high calcium fly ash geopolymer cured at ambient temperature. Materials and Design. 2014. 55. Pp. 58–65.
36. Adak, D., Sarkar, S., Mandal, S. Effect of nano silica on strength and durability of fly ash based geopolymer mortar. Construction and Building Materials. 2014. 70. Pp. 453–459.
37. Ibrahim, M., Megat Johari, M.A., Kalimur Rahman, M., Maslehuddin, M. Effect of alkaline activators and binder content on the properties of natural pozzolan-based alkali activated concrete. Construction and Building Materials. 2017. 147. Pp. 648–660. DOI: 10.1016/j.conbuildmat.2017.04.163
38. Ibrahim, M., Megat Johari, M.A., Maslehuddin, M., Kalimur Rahman, M. Influence of nano-SiO_2 on the strength and microstructure of natural pozzolan based alkali activated concrete. Construction and Building Materials. 2018. 173. Pp. 573–585.
39. Ibrahim, M., Megat Johari, M.A., Rahman, M.K., Maslehuddin, M., Hatim, D.M. Enhancing the engineering properties and microstructure of room temperature cured alkali activated natural pozzolan based concrete utilizing nanosilica. Construction and Building Materials. 2018. 189. Pp. 352–365.
40. Ibrahim, M., Megat Johari, M.A., Maslehuddin, M., Kalimur Rahman, M., Salami, B.A., Hatim Dafalla, M. Influence of composition and concentration of alkaline activator on the properties of natural-pozzolan based green concrete. Construction and Building Materials. 2019. 201. Pp. 186–195.
41. Ibrahim, M., Megat Johari, M.A., Hussaini, S.R., Kalimur Rahman, M., Maslehuddin, M. Influence of pore structure on the properties of green concrete derived from natural pozzolan and nanosilica. Journal of Sustainable Cement-Based Materials. 2020. Pp. 1–26.
42. ASTM C33-10, Standard Specification for Concrete Aggregates, ASTM International, West Conshohocken, PA, 2010.
43. ASTM C1437, 2010. Standard Test Method for Flow of Hydraulic Cement Mortar, ASTM International, West Conshohocken, PA.
44. ASTM C403, 2010. Standard Test Method for Time of Setting of Concrete Mixtures by Penetration Resistance, ASTM International, West Conshohocken, PA.
45. Ji, Y.L., Sun, Z.P., Yang, X. Assessment and mechanism study of bleeding process in cement paste by 1H low-field NMR. Construction and Building Materials. 2015. 100. Pp. 255–261.
46. Wang, Y., Yuan, Q., Deng, D., Ye, T., Fang, L. Measuring the pore structure of cement asphalt mortar by nuclear magnetic resonance, Construction and Building Materials. 2017. Pp. 450–458.
47. ASTM C109,2010, Standard Test Method for Compressive Strength of Hydraulic Cement Mortars (Using 2-in. or [50-mm] Cube Specimens), ASTM International, West Conshohocken, PA, 2010.
48. ASTM C78-10, Standard Test Method for Flexural Strength of Concrete (Using Simple Beam with Third-Point Loading), ASTM International, West Conshohocken, PA, 2010.
49. ASTM C469, 2010, Standard Test Method for Static Modulus of Elasticity and Poisson's Ratio of Concrete in Compression, ASTM International, West Conshohocken, PA, 2010.
50. ASTM C642, 2010. Standard Test Method for Density, Absorption, and Voids in Hardened Concrete, ASTM International, West Conshohocken, PA.

51. NTBUILD-492, NORDTEST METHOD: Concrete, Mortar And Cement-Based Repair Materials: Chloride Migration Coefficient From Non-Steady-State Migration Experiments. 2010.
52. Mallikarjuna Rao, G., Gunneswara Rao, T.D. Final Setting Time and Compressive Strength of Fly Ash and GGBS-Based Geopolymer Paste and Mortar. Arabian Journal for Science and Engineering. 2015. 40. Pp. 3067–3074.
53. ASTM C191, 2010. Standard Test Methods for Time of Setting of Hydraulic Cement by Vicat Needle, ASTM International, West Conshohocken, PA.
54. Teixeira-Pinto, A., Fernandes, P., Jalali, S. Geopolymer Manufacture and Application – Main problems when using concrete technology. Geopolymers. International Conference, Melbourne, 2002. Australia, Siloxo Pty. Ltd.
55. Fernández-Jiménez, A., Palomo, A. Composition and microstructure of alkali activated fly ash binder: effect of the activator. Cement and Concrete Research. 2005. 35(10). Pp. 1984–1992. DOI: 10.1016/j.cemconres.2005.03.003
56. Haha, M.B., Lothenbach, B., Le, S.G., Winnefeld, F. Influence of slag chemistry on the hydration of alkali-activated blast-furnace slag-Part II: Effect of Al_2O_3. Cement and Concrete Research. 2012. 42(1). Pp. 74–83. DOI: 10.1016/j.cemconres.2011.05.002
57. Deir, E., Gabreziabiher, B.S., Peethamparan, S. Influence of starting material on the early age hydration kinetics, microstructure and composition of binding gel in alkali activated binder systems. Cement and Concrete Composites. 2014. 48. Pp. 108–117. DOI: 10.1016/j.cemconcomp.2013.11.010
58. Gao, X., Yu, Q.L., Brouwers, H.J.H. Characterization of alkali activated slag–fly ash blends containing nano-silica. Construction and Building Materials. 2015. 98. Pp. 397–406.
59. Duxson, P., Fernández-Jiménez, A., Provis, J.L., Lukey, G.C., Palomo, A., Van Deventer J.S.J. Geopolymer technology: the current state of the art. Journal of Materials Science. 2007. 42(9). Pp. 2917–2933.
60. Yokoyama, Y., Yokoi, T., Ihara, J. The effects of pore size distribution and working techniques on the absorption and water content of concrete floor slab surfaces. Construction and Building Materials. 2014. 50(1). Pp. 560–566.
61. Rodriguez, E.D., Bernal, S.A., Provis, J.L., Paya, J., Monzo, J.M., Borrachero, M.V. Effect of nanosilica-based activators on the performance of an alkali-activated fly ash binder. Cement and Concrete Composites. 2013. 35. Pp. 1–11.
62. Zuo, Y., Ye, G. Pore structure characterization of sodium hydroxide activated slag using mercury intrusion porosimetry, nitrogen adsorption, and image analysis. Materials. 2018. 11. 1035. DOI: 10.3390/ma11061035
63. Shaikh, F., Chavda, V., Minhaj, N., Arel, H.S. Effect of mixing methods of nano silica on properties of recycled aggregate concrete. Structural Concrete. 2019. 19(2). Pp. 387–399.
64. Juhyuk, M.A., Sungchul, B.B., Celik, K.B., Yoon, S.B., Ki-Hyun, K.B., Kang, S.K.C., Paulo, J.M., Monteiro, B. Characterization of natural pozzolan-based geopolymeric binders. Cement and Concrete Composites. 2014. 53. Pp. 97–104.
65. Chen, W., Li, B., Li, Q., Tian, J. Effect of polyaluminum chloride on the properties and hydration of slag cement paste. Construction and Building Materials. 2016. 124. Pp. 1019–1027.
66. Li, Z., Wang, H., He, S., Lu, Y., Wang, M. Investigations on the preparation and mechanical properties of the nano-alumina reinforced cement composite. Materials Letters. 2006. 60. Pp. 356–359.
67. Barbhuiya, S., Mukherjee, S., Nikraz, H. Effects of nano-Al_2O_3 on early-age microstructural properties of cement paste. Construction and Building Materials. 2014. 52. Pp. 189–193.
68. Provis, J.L., van Deventer, J.S.J. Geopolymers: structures, processing, properties and industrial applications. Elsevier, 2009.
69. Yip, C.K., Lukey, G.C., Van Deventer, J.S.J. Coexistence of geopolymeric gel and calcium silicate hydrate at the early stage of alkali activation. Cement and Concrete Research. 2005. 35. Pp. 1688–1697.
70. Yip, C.K., Van Deventer, J.S.J. Microanalysis of calcium silicate hydrate gel formed within a geopolymeric binder. Journal of Material Science 2003. 38. Pp. 3851–3860.
71. Thomas, R.J., Ariyachandra, E., Lezama, D., Peethamparan, S. Comparison of chloride permeability methods for Alkali-Activated concrete. Construction and Building Materials. 2018. 165. Pp. 104–111.
72. Ravikumar, D., Neithalath, N. An electrical impedance investigation into the chloride ion transport resistance of alkali silicate powder activated slag concretes. Cement and Concrete Research. 2013. 44. Pp. 58–68.

Contacts:

Mohammed Ibrahim, ibrahim@kfupm.edu.sa

Muhammad Nasir, mnmuhammad@iau.edu.sa

Syed Rizwanullah Hussaini, rsyed@kfupm.edu.sa

Syed Khaja Najamuddin, sknajam@kfupm.edu.sa

Adeoluwa Ewebajo, adeoluwaewebajo@gmail.com